

## Original Article

---

# Lysate Array Analyses of Signal Transduction Inhibitors in Tumor Cell Lines

Victor A. Levin,<sup>1,\*</sup> Kenji Tada,<sup>1</sup> and Cristian Mircean<sup>2</sup>

Departments of <sup>1</sup>Neuro-Oncology and <sup>2</sup>Pathology, The University of Texas M.D. Anderson Cancer Center, Houston, TX

### Abstract

We probed the ability of reverse lysate array technology to help explain potential differences in the responses of cancer cells to various small-molecule kinase inhibitors. To understand the antitumor potential of signal transduction inhibitors and their effects on signaling pathways downstream of Src, we used reverse lysate array technology to study SIG11293, a selective inhibitor of Src and Lck kinases, and AEE788, a selective inhibitor of Kdr (VEGFR1) and epidermal growth factor receptor/ErbB-2 that also has affinity for Src, c-abl, c-fms, and Flt-1. We observed the effects of drug dose on cell killing and expression and phosphorylation of various signal transduction proteins in MDA435 and MDA231 human breast cancer cells and U251HF glioblastoma cells. After 24 h, SIG11293 induced the least amount of cell killing in MDA435 cells;

decreased Stat3(pY705) and Src(pY529) in all cell lines; decreased Src(pY418) and total Src in MDA231 and MDA435 cells, but not U251 cells; and in U251 cells, uniquely increased activated caspase 3, Src(pY418), panSrc, and p70S6K. AEE788 decreased Src(pY529) and Stat3(pY705) in U251HF and MDA435 cells. In regard to Src phosphorylation, both drugs decreased the negative regulatory site, Src (pY529), more than the positive regulatory site, Src(pY418), relative to total Src. These observations suggest that the two drugs have complex and different effects on Src signaling pathways. Although this general conclusion could be predicted, we believe that these studies exemplify the ability and robustness of reverse lysate arrays to measure signaling pathway modulation in tumor cells. Our hope is that these techniques will help to develop more robust preclinical and, eventually, clinical treatment paradigms.

\*Author to whom all correspondence and reprint requests should be addressed:  
Victor A. Levin, Neuro-Oncology Unit 431, The University of Texas  
M.D. Anderson Cancer Center, P.O. Box 301402, Houston, TX 77230-1402.  
E-mail: vlevin@mdanderson.org.

**Key Words:** Quantitative lysate arrays; phosphospecific antibodies; AEE788; SIG11293; Src.

## Introduction

The therapeutic potential of small-molecule drug inhibitors of specific signaling pathways largely is assessed by their affinity to a target or group of targets. A drug is deemed to be specific with respect to target and mode of action *in vitro* if there is at least one order of magnitude difference between its affinity with or response from the main target compared with its affinity to or response from other possible targets. Unfortunately, it is often difficult to assess a drug's function within a particular tumor because of the potential for nonlinear interactions among signaling molecules, the unknown time- and dose-dependent changes in signal transduction caused by the drug, the inherent pharmacodynamic and pharmacokinetic heterogeneity in response to the drug, and the inherent heterogeneity of tumor cell functions.

Although the recently developed small-molecule inhibitors of receptor and non-receptor protein tyrosine kinases (PTKs) are attractive conceptually, they are far from specific or selective in their abilities to inhibit the kinases in a constant manner and with a constant outcome. The relative differences between the affinities of the inhibitors for their target kinases *in vitro* often do not reflect their inhibitory values for enzymes in cells. Indeed, small-molecule inhibitors cannot be easily tested against all potentially competing kinases in cells, let alone *in situ* in the tumor of interest. This problem is more apparent in the case of receptor and nonreceptor PTK inhibitors, as signaling pathways within cells of different tumors interact variably when confronted with the many intra- and extracellular influences. Even in cultured cells, the response to a PTK inhibitor can produce disparate effects depending on the dose of inhibitor, length of exposure to the drug, and inherent genetic instability of tumor cells.

These aforementioned difficulties are likely to account for some of the variable responses of patients to targeted therapies and strongly suggest that profiling the targeted kinases and their associated pathways in tumor cells is crucial to a rational understanding of tumor response to inhibitors. Thus, in an effort to better define the similarities and differences among cancer cell lines and between small-molecule kinase inhibitors, we initiated the reverse lysate array studies of kinase inhibitors presented in this article.

The inhibitors used in this study were selected for their ability to inhibit Src-kinase activity. SIG11293, a thienopyrimidine, was chosen because it is a primary Src-kinase inhibitor, although it does have a similar half-maximal inhibitory concentration for Lck (1). AEE788, a 7H-pyrrolo-[2,3-D]-pyrimidine inhibitor, was chosen because it primarily inhibits Kdr (VEGFR1) and epidermal growth factor receptor (EGFR)/ErbB-2 kinase activity and has lower half-maximal inhibitory concentration values for Src, c-abl, c-fms, and Flt-1 (2). The use of reverse lysate arrays to probe changes in protein and phosphoprotein expression was predicated on its potential to study, in a semiquantitative manner, non-denatured cellular proteins from cultured tumor cells. Although reverse lysate arrays have been used to analyze cancer cells from tissue, cultured cells, cells treated with drugs, and T-lymphocytes (3), use of reverse lysate arrays in the field of cancer research remains relatively young. An encouraging study by Herrmann et al. (4) used this technology to assess the mitochondrial proteome in prostate cancer. In that study, reverse lysate arrays, Western blots, and immunohistochemistry were used to examine mitochondrial cytochrome *c* oxidase levels in four prostate carcinoma and six other cancer biopsy samples in an effort to better understand the malignant phenotype. In another study, Chan et al. (5) used reverse-phase lysate microarrays to probe specific

protein phosphorylation in 62 signaling sites in stimulated Jurkat T cells. Last, Utz wrote a scholarly review of protein arrays and their application for the study of blood cells and their secreted products; he expects array technology will markedly influence immunology research in the fields of autoimmunity and inflammation (3).

We used the quantitative reverse lysate array technology to evaluate the ability of SIG11293 and AEE788 to effect cell killing and changes in representative proteins and phosphoproteins in three cancer cell lines. The experiments presented provide a strategy for profiling kinases and inhibitors using discrete tumor cell lines.

## Materials and Methods

### Cell Cultures

We used two human breast carcinoma lines, MDA435 and MDA231 (gift from Francisco Esteva, The University of Texas M.D. Anderson Cancer Center), that differ in their degree of malignancy (6), ability to metastasize in nude mice (7), and sensitivity to Src inhibitors (8). We also used the U251HF human glioblastoma multiforme cell line (a gift from Juan Fueyo, The University of Texas M.D. Anderson Cancer Center), which responds to Src inhibitors through an apoptotic pathway (8). Our choice of cell lines was based partly on their disparate levels of dependence on Src kinase pathways and sensitivities to inhibitors of Src and other signal transduction molecules.

U251HF cells were maintained in Dulbecco's modified essential/F12 medium supplemented with 5% fetal bovine serum (FBS). MDA435 and MDA231 cells were maintained in Leibovitz's L-15 medium supplemented with 5% FBS.

K562 chronic myelogenous leukemia cells (9) (a gift of Nicholas Donato, The University of Texas M.D. Anderson Cancer Center) served as

negative control cells for all Src antibodies and were grown in RPMI 1640 medium. SW480 colon cancer cells (a gift from Gary Gallick, The University of Texas M.D. Anderson Cancer Center) transfected with an expression plasmid (c-srcY527F) expressing constitutively active Src (10) served as the positive control cell for all Src antibodies and were maintained in Leibovitz's L-15 medium supplemented with 5% FBS.

### Drugs

SIG11293, a thienopyrimidine with a molecular weight of 434, was a gift from Raymond Budde (Signase, Houston, TX). AEE788, a 7H-pyrrolo-[2,3-D]-pyrimidine with a molecular weight of 441, was a gift from Novartis Pharmaceutical Research (Princeton, NJ). Both drugs were dissolved in dimethylsulfoxide and stored as 5 mg/mL stock solutions at room temperature.

### Lysis Buffer

The lysis buffer stock solution was prepared in 50-mL volumes using 1 mL of 1 M Tris-HCl (pH 7.6; final concentration of 20 mM), 1.5 mL of 5 M NaCl (final concentration of 150 mM), 0.5 mL of 0.5 M EDTA (pH 8.0; final concentration of 5 mM), and 46.75 mL of double-distilled water. The solution was filtered, autoclaved, and stored at 4°C. Immediately before lysing the cells, we added to the stock solution five protease inhibitor cocktail tablets (EDTA-free complete mini-tablets; Roche Applied Science, Indianapolis, IN), 10.5 mg of 5 mM sodium fluoride, 9.2 mg of 1 mM sodium orthovanadate, 115 mg of 5 mM sodium pyrophosphate, and 250 µL of Igepal CA-630 to make a 0.5% solution.

### Primary Antibodies

Commercial rabbit polyclonal antibodies were used to detect Tyr418-phosphorylated Src (Src[pY418]; 1:250), Src(pY529) (1:250), panSrc (1:250), and Stat3(pY705) (1:250; all from Biosource International, Camarillo, CA);

and p38MAPK(pY180/pY182) (1:250) and p70S60K(pT389) (1:250; both from Cell Signaling Technology, Beverly, MA). Monoclonal rabbit antibody was used to detect active caspase 3 (1:100; BD Biosciences, Palo Alto, CA). Polyclonal rabbit antibody against  $\beta$ -actin (1:1000; Santa Cruz Biotechnology, Santa Cruz, CA) was used as a positive control. Primary antibody was omitted as a negative control. We confirmed that all primary antibodies had only one dominant band, except for activated caspase-3, which had two bands as expected.

### **Cell Counts**

U251HF, MDA231, and MDA435 cells ( $1 \times 10^4$  each) were seeded on 24-well plates with Dulbecco's modified essential/F12 medium or Leibovitz's medium supplemented with 5% FBS and incubated for 24 h. The following day, the medium was replaced with FBS-free medium containing SIG11293 and AEE788 at various concentrations (0.1, 1, and 10  $\mu$ M).

For cell counting, the cells were incubated with the drugs for 24 h and then trypsinized, suspended in phosphate-buffered saline, and counted using a Vi-Cell cell viability analyzer (Beckman Coulter, Fullerton, CA). The data were analyzed by averaging triplicate values for each treatment and calculating the ratios of treated to untreated cell numbers for all doses and cell lines tested using the equation, cell kill =  $(1 - \text{treated cell number}/\text{control cell number}) \times 100$ .

### **Preparation of Samples for Microarray Analysis**

To prepare cell lysates for microarray experiments, cells were plated in flasks on sequential days. Concentrations were maintained at  $10^6$  cells/mL or less to avoid natural induction of apoptosis by cell confluence. Cells were harvested using 0.25% trypsin and counted, and  $5 \times 10^6$  cells were transferred into a 6-well

plate (35-mm diameter, 5-mL volume) and incubated for 24 h at 37°C in 5% CO<sub>2</sub>. SIG11293 and AEE788 were added to the medium at 0.1, 1.0, and 10  $\mu$ M, and the cells were again incubated for 24 h at 37°C in 5% CO<sub>2</sub>. The cells were then harvested by scraping and transferred with medium into 15-mL tubes (BD Falcon, Franklin Lakes, NJ) on ice and spun for 5 min at 4°C and 16,100g. The medium was removed and discarded, and the remaining cells were lysed with 0.5-mL lysis buffer on ice and mixed by pipetting. After 30 min on ice, the tubes were spun for 20 min at 4°C and 16,100g. Fifty microliters of supernatant from each tube were transferred to a 96-well plate (Eppendorf, Westbury, NY), and the plates were stored at -80°C until use.

### **Reverse-Phase Protein Lysate Microarray Printing**

Slides of six dilutions of each of the samples in triplicate were made by a liquid-handling RSP robot (TECAN US, Research Triangle Park, NC). The dilutions were then spotted onto nitrocellulose-coated FAST slides (Scheicher and Schuell, Keene, NH) with a 500- $\mu$ m center-to-center interspot distance using a G3 spotter (Genomics Solutions, Ann Arbor, MI). Triplicate spots of each dilution point were produced, with six transfers for each dilution.

### **Detection and Imaging**

A heavily modified catalyzed signal amplification kit (cat. no. K1500; DakoCytomation, Carpinteria, CA) was used to detect target proteins. Briefly, the slides were blocked with Re-Blot Plus mild solution (cat. no. 2502; Chemicon, Temecula, CA) and then blocked overnight with I-block (cat. no. Tropix AI300; Applied Biosystems, Foster City, CA). Blocking was continued the following day with fresh 3% hydrogen peroxide, avidin/biotin, and casein. Primary antibodies were diluted in antibody dilution buffer and incubated with the slides at

25°C for 1 h in a humidified chamber. Secondary biotinylated antirabbit (BA-1000) or antimouse (BA-9200) antibodies (Vector Laboratories, Burlingame, CA) were diluted 1:10,000 and incubated with the slides at 25°C for 1 h. The slides were then incubated with streptavidin/biotin, amplification reagent, and streptavidin/peroxidase from the kit followed by development with DAB+ (Dako). After each step, the slides were washed with 0.1% Tris-buffered saline containing Tween (pH 7.4) to remove the previous reagents. The slides were scanned in color at 1200 dots per inch; the resulting image was converted to a 16-bit grayscale image and inverted to allow quantification by ArrayVision software (Imaging Research, St. Catharines, Ontario, Canada).

### Analysis of Relative Amounts of Primary Antibodies

Lysate arrays are more susceptible than microarrays to artifacts, such as saturation, membrane irregularities, or improper spot segmentation. To estimate a single value for each sample (defined as lysate expression), we used an exponential least-squares fit ( $Y = A^{BX}$ ) to fit the 18 spots (sixfold dilutions with three replicates for each dilution). In most cases, our data easily fit a simple exponential least-squares plot of the intensity vs 1-dilution, in which the dilutions ranged from 1:1 to 1:32 (1 to 0.03125). Variance was typically 10% or less. **Figure 1** shows a representative plot of the triplicate data points at each of the six dilutions for a 10  $\mu\text{M}$  dose of SIG11293 in MDA231 cells probed with anti-Src(pY418) antibody.

Signal intensity was measured relative to one of the samples, which was chosen as a reference to obtain optimal results. To preserve the optical constraints of common samples, the spots for the reference sample were acquired in a linear range of nonsaturated dilutions (11). The distance between the two fitted lines in log-log space was calculated from the actual ratios between the current samples and the

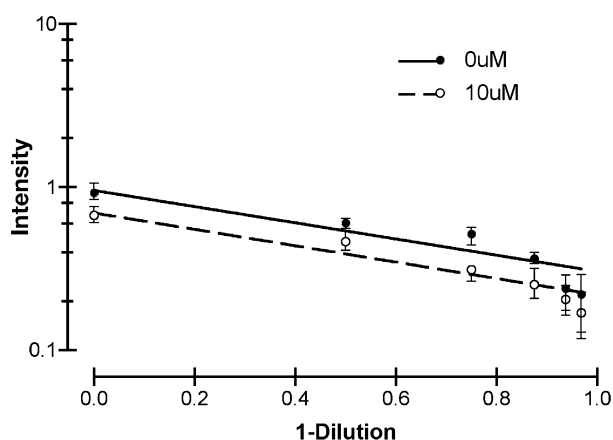


Fig. 1. Intensity of staining with anti-Src(pY418) antibody at 1:1, 1:4, 1:8, 1:16, and 1:32 dilutions in MDA231 cells treated with 0 or 10  $\mu\text{M}$  SIG11293. Data shown are means  $\pm$  standard error of triplicate values. No distance corrections were made. Exponential least squares fitting to all 0  $\mu\text{M}$  data points (—) was done using the equation  $Y = 0.956^{-1.142X}$  with  $R^2 = 0.88$ ; fitting for 10  $\mu\text{M}$  points (- -) was done using  $Y = 0.695^{-1.156X}$  with  $R^2 = 0.91$ .

references. We chose the sample of MDA435 cells treated with 10  $\mu\text{M}$  AEE788 because the behavior of its nonsaturated spots was superior with respect to linearity of signal intensity compared to that of samples treated with the other primary antibodies.

Signal intensity was normalized to that of  $\beta$ -actin (positive control) and ranged from 0.944 to 1.062. Because the levels of phosphorylated and nonphosphorylated signaling proteins differed in each of the three cell lines, we used the expression levels for each cell line and drug dose to calculate a Pearson correlation matrix highlighting relationships among the various primary antibodies.

## Results

### Cell Killing

At the doses used, each drug produced only modest effects on cell killing. These data are summarized in **Table 1** for the three cell lines. Of interest is the observation that the effect

Table 1  
Cell Killing Induced by SIG11293 and AEE788  
in Three Cell Lines at 24 h<sup>a</sup>

	Dose $\mu$ M	% Cell kill	
		SIG11293	AEE788
U251HF	0	0	0
	0.1	12	6
	1	68	3
	10	69	33
MDA435	0	0	0
	0.1	-8	50
	1	25	42
	10	50	42
MDA231	0	0	0
	0.1	0	0
	1	50	21
	10	78	33

<sup>a</sup>Cell kill =  $(1 - \text{treated cell number}/\text{control cell number}) \times 100$ .

of SIG11293 on cell killing was greatest in MDA231 cells and least on MDA435 cells, whereas for AEE788, it was greatest in MDA435 cells and equal in U251HF and MDA231 cells. These data imply that the two drugs produce their effects on cell killing by somewhat dissimilar means. In no case did we see the type of cell killing observed with cytotoxic alkylating agents where dose-dependent log cell kill is typically observed.

### Reverse Lysate Array

The data obtained for the two drugs were quite similar with respect to the intensity of antibody staining. The data for normalization of the intensities of the primary antibodies to that of the control  $\beta$ -actin antibody are shown in Table 2. There was good internal agreement among the cell lines and drug groups. However, there appeared to be differences among the cell lines in the absolute levels of Src(pY418), Src(pY529), panSrc, Stat3(pY705), activated caspase-3, p38MAPK, and p70S6K proteins. U251HF cells had

lower absolute values than did MDA231 and MDA435 cells, which appeared to be similar with respect to these proteins.

After treatment with the two drugs, changes were observed with respect to the amounts of specific proteins and phosphoproteins. To compare changes in the proteins with respect to increasing drug dose, cell line, and drug, the following formula was used:

$$P = (1 - I_t/I_c) \times 100 \quad (1)$$

in which  $P$  is percent change,  $I_t$  is intensity of drug-treated sample, and  $I_c$  is intensity of control sample (no drug).

Table 3 shows that, exclusive of  $\beta$ -actin, the seven proteins varied from their control intensities in different ways in response to the drugs. To simplify viewing, the mean change in protein is shown with its  $p$ -value for the change based on a  $t$ -test for sample means. For SIG11293, the effect on the three cell lines was directionally down for Src(pY529) and Stat3(pY705). Although it was up in the three cell lines for p38MAPK, it was most prominent in the U251 cells ( $p = 0.01$ ). U251 was also unique in that this cell line was the only one to increase panSrc and Src(pY418) levels (neither significant) in response to SIG11293. AEE788 increased Stat3(pY705) significantly ( $p = 0.002$ ) in MDA435 cells but to a lesser extent in the other cell lines. Activated caspase 3 increased in all lines, p38MAPK in U251 and MDA435 cells. AEE788 increased panSrc in U251 and MDA435 cells and increased Src(pY418) in all cell lines.

The relationship between these directional changes in protein levels, the dose of each drug, and the cell line used were evaluated using a Pearson correlation matrix (summarized in Table 4). The correlation coefficients ranged from -1 (inverse relationship) to +1 (direct relationship); 0 indicated the absence of a linear relationship. The closer the coefficient approaches +1 or -1 the more significant the correlation to direct or inverse movement

Table 2  
Normalization of Initial Antibody Intensity to  $\beta$ -Actin for the Two Separate Drug Studies<sup>a</sup>

Cell line	Relative antibody intensity						
	Src (pY418)	Src (pY529)	panSrc	Stat3 (pY705)	Activated caspase 3	p38MAPK	p70S6K
U251HF	0.317	0.677	0.195	0.140	0.144	0.290	0.135
	0.365	0.671	0.247	0.154	0.140	0.292	0.116
Mean	0.341	0.674	0.221	0.147	0.142	0.291	0.126
MDA435	0.482	0.836	0.364	0.402	0.193	0.582	0.174
	0.480	0.827	0.358	0.433	0.192	0.562	0.166
Mean	0.481	0.832	0.361	0.418	0.193	0.572	0.170
MDA231	0.467	0.755	0.373	0.403	0.200	0.475	0.163
	0.424	0.749	0.353	0.376	0.194	0.517	0.171
Mean	0.446	0.752	0.363	0.390	0.197	0.496	0.167

<sup>a</sup>The cell lines are nominally ordered by increasing intensity.

of the protein relative to the increase of drug dose.

## Discussion

Our data show some differences in the effects of SIG11293, a primary Src-kinase inhibitor, and AEE788, a primary EGFR/ ErbB-2 kinase inhibitor and secondary Src-kinase/Abl-kinase inhibitor. We found that AEE788 was modestly better than SIG11293 at cell killing and that although the two drugs shared some features with regard to protein and phosphoprotein levels, there were major differences in Stat3(pY705), Src(pY418), and Src(pY529) levels. As expected, SIG11293 was selective for Src kinase, had nearly equal activity against Lck, and had less than 10% of Src activity against other Src-family kinases, EGFR, and platelet-derived growth factor receptor (1). In contrast, AEE788 inhibited Kdr, EGFR/ ErbB-2, Src, c-abl, c-fms, and Flt-1, with a 30-fold greater effect against EGFR and a 10-fold greater effect against ErbB2 compared with Src (2). Because Kdr is not especially important in the cultured cell lines studied here, we surmised that other targets, such as EGFR, Src, c-abl, and c-fms, would be the

more likely functional targets of AEE788 in our monolayer culture studies.

The Pearson correlation matrices (Table 4) indicate that SIG11293 produces two common effects on all three cell lines: decreased Stat3(pY705) and Src(pY529). In our analysis, correlation coefficients greater than 0.95 were considered significant at  $p < 0.05$ ; however, we believe that it is also of value to look at trends for which the correlation coefficient is +0.70 or more or -0.70 or less. The added insight from these observations is that the three cell lines appeared to differ somewhat in their responses to increasing doses of SIG11293: MDA435 cells showed decreased p38MAPK; U251HF cells showed a unique increase in activated caspase 3, panSrc, Src(pY418), and p70S6K; and MDA231 cells showed no additional changes in protein expression or phosphorylation although Src(pY418) appeared to trend down. For AEE788, the trends in protein expression and phosphorylation had few similarities among the three cell lines. For MDA435 cells, AEE788 did not have any significant effect ( $\geq +0.70$  or  $\leq -0.70$ ) on expression or phosphorylation of any of the proteins; this may indicate that AEE788 acts more through

Table 3  
 Effect of SIG11293 and AEE788 Dose on Percent Change (P) for Individual Antibodies (Normalized With  $\beta$ -Actin) Without Drug Exposure (0  $\mu$ M Dose) to the Three Doses of Each Drug for Three Cell Lines<sup>a</sup>

Cell line	Dose, $\mu$ M	Percent change ( $(I - I_0/I_0) \times 100$ )																
		SIG11293						AEE788										
		% Cell kill	Src (pY418)	Src (pY529)	Src	Stat3 (pY705)	Activated caspase 3	p38 MAPK	p70 S6K	% Cell kill	Src (pY418)	Src (pY529)	Src	Stat3 (pY705)	Activated caspase 3	p38 MAPK	p70 S6K	
U251	0	0	0	0	0	0	0	0	0	0	0	0	0	0	0	0	0	0
	0.1	12	16	-20	45	-7	70	50	18	6	26	13	54	38	84	70	62	
	1	68	10	-9	19	-6	9	46	5	30	4	5	6	11	16	7	9	
MDA435	10	69	34	-28	79	-35	94	63	43	33	14	-19	58	-12	113	43	59	
	mean		20	-19	48	-16	58	53	22		15	0	40	12	71	40	43	
	p-value		0.11	0.08	0.11	0.24	0.15	0.01	0.19		-0.13	-0.42	-0.32	-0.50	-0.52	-0.40	-0.32	
MDA231	0	0	0	0	0	0	0	0	0	0	0	0	0	0	0	0	0	
	0.1	-8	27	4	43	15	71	51	35	50	37	18	58	48	78	63	61	
	1	25	-14	-25	-26	-23	-1	38	-25	42	3	-4	12	20	3	-10	14	
MDA231	10	50	-18	-49	-19	-77	36	-29	2	42	12	-5	44	41	97	16	70	
	mean		-2	-23	-1	-29	35	20	4		17	3	38	36	59	23	48	
	p-value		0.91	0.26	0.98	0.40	0.23	0.51	0.83		-0.27	-0.29	-0.21	0.002	-0.64	-0.70	-0.26	
MDA231	0	0	0	0	0	0	0	0	0	0	0	0	0	0	0	0	0	
	0.1	0	12	-05	25	0	58	84	37	0	18	7	36	17	49	55	39	
	1	50	-20	-27	-31	-32	-8	5	-20	21	3	0	-8	7	-2	-15	9	
MDA231	10	78	-22	-52	-20	-79	23	-16	-3	33	4	-10	14	-8	64	2	47	
	mean		-10	-28	-9	-37	24	25	5		8	-1	14	5	37	14	32	
	p-value		0.47	0.18	0.66	0.25	0.33	0.50	0.81		-0.12	-0.23	-0.40	-0.26	-0.48	-0.77	-0.18	

<sup>a</sup>Only bolded p-values are significant by the t-test for sample means.

Table 4  
The Pearson Correlation Matrix for the Effect of SIG11293 or AEE788 on Each Cell Line<sup>a</sup>

SIG11293		AEE788	
U251HF (69%)	Coefficient	U251HF (33%)	Coefficient
Dose	1	Dose	1
p70S6K	0.91	Cell kill	0.98
Src (pY418)	0.89	Activated caspase 3	0.72
panSrc	0.84	panSrc	0.60
Activated caspase 3	0.71	p70S6K	0.52
Cell kill	0.65	p38MAPK	0.23
p38MAPK	0.61	Src (pY418)	0.16
Src (pY529)	-0.75	Stat3 (pY705)	-0.68
Stat3 (pY705)	-0.98	Src (pY529)	-0.92
MD435 (50%)	Coefficient	MD435 (42%)	Coefficient
Dose	1	Dose	1
Cell kill	0.89	Activated caspase 3	0.67
Activated caspase 3	0.14	p70S6K	0.64
p70S6K	-0.09	Stat3 (pY705)	0.43
panSrc	-0.45	panSrc	0.36
Src (pY418)	-0.61	Cell kill	0.29
p38MAPK	-0.78	Src (pY418)	-0.06
Src (pY529)	-0.90	p38MAPK	-0.08
Stat3 (pY705)	-0.95	Src (pY529)	-0.49
MDA231 (78%)	Coefficient	MDA231 (33%)	Coefficient
Dose	1	Dose	1
Cell kill	0.85	Cell kill	0.85
Activated caspase 3	0.06	Activated caspase 3	0.68
p70S6K	-0.25	p70S6K	0.66
panSrc	-0.44	panSrc	0.07
p38MAPK	-0.54	Src (pY418)	-0.20
Src (pY418)	-0.64	p38MAPK	-0.24
Src (pY529)	-0.91	Stat3 (pY705)	-0.74
Stat3 (pY705)	-0.95	Src (pY529)	-0.90

<sup>a</sup>Values in parentheses are the cell kill 24 h after 10  $\mu$ M of drug exposure.

the Ras and MAPK pathways because it inhibits EGFR/ErbB-2. For U251HF cells, there was a decrease in Src(pY529) and increase in activated caspase-3. In MDA231 cells, there was a decrease in Src(pY529) and Stat3(pY705). Although the Pearson correlation coefficients were not always less than -0.70, activated caspase-3 appears to have increased in all cell lines in response to

AEE788, but only in U251HF cells in response to SIG11293. Thus, the data in [Tables 1, 3, and 5](#) suggest that the signaling mechanisms responsible for the cell killing induced by AEE788 is related to caspase-3-mediated apoptosis and only for U251HF in the case of SIG11293.

Because both drugs inhibit Src kinase, we compared the effects of the highest dose

Table 5  
Effects of 10  $\mu\text{M}$  SIG11293 and AEE788 on Src Phosphorylation<sup>a</sup>

Drug	Cell line	Percent change ( $[1 - I_t/I_c] \times 100$ )			
		$\beta$ -Actin normalized		panSrc normalized	
		Src (pY418)	Src (pY529)	Src (pY418)	Src (pY529)
SIG11293	U251	34	-28	-25	-60
AEE788	U251	14	-19	-28	-49
SIG11293	MDA435	-18	-49	1	-37
AEE788	MDA435	12	-5	-22	-34
SIG11293	MDA231	-22	-52	-2	-40
AEE788	MDA231	4	-10	-9	-22

Changes between control (0  $\mu\text{M}$ ) and the 10  $\mu\text{M}$  dose normalized with  $\beta$ -actin or panSrc proteins are shown.

(10  $\mu\text{M}$ ) of each drug on Src (Table 5). Under those conditions, there appears to be some commonality in the direct effects of the two drugs on Src kinase. When looking at Src autophosphorylation, if the amounts of Src(pY418) and Src(pY529) were normalized to that of panSrc, then Src(pY529), the negative regulatory site of activated Src, was decreased by both drugs to a greater extent than was Src(pY418), the positive regulatory site of activated Src. Thus, it can be appreciated that one would have a false impression of the impact of both drugs on Src(pY418) if only  $\beta$ -actin normalization was used and no consideration was given to the rising Src protein (panSrc) level in the one cell line. From a mechanistic point of view, these Src-phosphoprotein observations will require further study with other Src-kinase inhibitors.

The biological effects of the two drugs on the three cell lines are still not fully understood. Our observations pertain only to cells in culture, so we do not know whether the perturbations in signal transduction would be the same in a tumor *in situ*. Unfortunately, it is much more difficult today to study drugs' effects on solid tumors using reverse lysate arrays because of the amount of protein required for the current generation of detection instruments. We

believe, however, that our findings show the benefit of reverse lysate arrays in studying the quantitative effects of drugs on signaling pathways. We are expanding these studies to examine a wider variety of proteins in cultured cells, and we are developing techniques for replicating our studies in xenografts of the same three tumor cell lines. It is hoped that the added insights from these expanded experiments will aid in the design of better chemotherapies for cancer patients.

### Acknowledgments

The authors thank Pierrette Lo, BA for editorial assistance, David E. Cogdell for preparation of arrays and help with slide staining, Patricia Koch, MS for cell kill studies, and Kevin R. Coombes, PhD for advice concerning statistical methods appropriate to the presentation of study results. These studies were supported in part by the Alan Gold Memorial Fund, the Lester Heath Fund, and the Bullock Family Fund.

### References

1. Budde, R. J. (2003) Effect of thienopyrimidines on Src kinases and cultured cancer cells. Corporate Report. Houston: Signase Inc.
2. Traxler, P., Allegrini, P. R., Brandt, R., et al. (2004) AEE788: a dual family epidermal

- growth factor receptor/ErbB2 and vascular endothelial growth factor receptor tyrosine kinase inhibitor with antitumor and antiangiogenic activity. *Cancer Res.* **64**, 4931–4941.
3. Utz, P. J. (2005) Protein arrays for studying blood cells and their secreted products. *Immunol. Rev.* **204**, 264–282.
  4. Herrmann, P. C., Gillespie, J. W., Charboneau, L., et al. (2003) Mitochondrial proteome: altered cytochrome c oxidase subunit levels in prostate cancer. *Proteomics* **3**, 1801–1810.
  5. Chan, S. M., Ermann, J., Su, L., Fathman, C. G., and Utz, P. J. (2004) Protein microarrays for multiplex analysis of signal transduction pathways. *Nat. Med.* **10**, 1390–1396.
  6. Zhang, R. D., Fidler, I. J., and Price, J. E. (1991) Relative malignant potential of human breast carcinoma cell lines established from pleural effusions and a brain metastasis. *Invasion Metastasis* **11**, 204–215.
  7. Price, J. E., Polyzos, A., Zhang, R. D., and Daniels, L. M. (1990) Tumorigenicity and metastasis of human breast carcinoma cell lines in nude mice. *Cancer Res.* **50**, 717–721.
  8. Wong, E. T., Yung, W. K. A., Fueyo, J., et al. (1997) Induction of apoptosis in glioma cells by a benzodiazepin-2-one. *J. Neuro-oncol.* **35**, S49.
  9. Zinner, R. G., Nemunaitis, J. J., Donato, N. J., et al. (2001) A phase 1 clinical and biomarker study of the novel pan-erbB tyrosine kinase inhibitor, CI-1033, in patients with solid tumors. *Clin. Cancer Res.* **7**, 3767S–3768S.
  10. Allgayer, H., Wang, H., Gallick, G. E., et al. (1999) Transcriptional induction of the urokinase receptor gene by a constitutively active Src. Requirement of an upstream motif (-152/-135) bound with Sp1. *J. Biol. Chem.* **274**, 18,428–18,437.
  11. Mircean, C., Shmulevich, I., Cogdell, D., et al. (2005) Robust estimation of protein expression ratios with lysate microarray technology. *Bioinformatics* **21**, 1935–1942.